Biochemical Pharmacology 79 (2010) 842–852

Contents lists available at ScienceDirect

Biochemical Pharmacology

journal homepage: www.elsevier.com/locate/biochempharm

Reverse phase protein array identifies novel anti-invasion mechanisms of YC-1

Bo Hong [a,1], Vivian W.Y. Lui [a,b,1], Edwin P. Hui [c], Yiling Lu [d], Horasis S.Y. Leung [c], Elaine Y.L. Wong [a], Suk-Hang Cheng [e], Margaret H.L. Ng [e], Gordon B. Mills [d], Anthony T.C. Chan [c,*]

[a] Cancer Signaling Laboratory, Department of Clinical Oncology, The Chinese University of Hong Kong, Hong Kong
[b] Cancer Drug Testing Unit, State Key Laboratory of Oncology in South China, Department of Clinical Oncology, The Chinese University of Hong Kong, Hong Kong
[c] Department of Clinical Oncology, Sir YK Pao Center for Cancer, Hong Kong Cancer Institute and Li Ka Shing Institute of Health Sciences, The Chinese University of Hong Kong, Hong Kong
[d] Department of Systems Biology, University of Texas M.D. Anderson Cancer Center, Houston, TX, USA
[e] Department of Anatomical and Cellular Pathology, The Chinese University of Hong Kong, Hong Kong

ARTICLE INFO

Article history:
Received 15 September 2009
Accepted 22 October 2009

Keywords:
Anti-invasion
Anti-proliferation
Nasopharyngeal carcinoma (NPC)
Reverse phase protein array
YC-1 mechanisms

ABSTRACT

YC-1 has recently been demonstrated to have potent anti-invasion and anti-metastatic activity in several cancer models, in addition to its anti-proliferation activity. However, the mechanism underlying its anti-invasion/anti-metastatic activity is largely unknown. Nasopharyngeal carcinoma (NPC) is a highly metastatic head and neck cancer in Southeast Asia. Here, we demonstrated that YC-1 inhibited invasiveness and proliferation of NPC cells, with the latter being accompanied by PARP cleavage, S-phase arrest and activation of Chk1/Chk2. We aimed at identifying novel anti-invasion mechanisms of YC-1 in NPC by a functional proteomic platform, the reverse phase protein array (RPPA). Our study revealed for the first time that multiple invasion-related signaling proteins (β-catenin, caveolin, Src and EGFR), as well as several growth-related proteins (AMPKα, phospho-acetyl-CoA carboxylase (p-ACC), HER-2 and mTOR), which were previously un-described signaling proteins altered by YC-1, were found to be down-modulated by YC-1 in NPC cells. We hypothesized that YC-1-mediated downregulation of these invasion proteins contributed to its anti-invasion activity in NPC cells. Overexpression of EGFR, activated Src or caveolin, but not β-catenin reversed the inhibitory effects of YC-1 on NPC cell invasion, with EGFR and activated Src having additional effects on rescuing NPC cells from YC-1-mediated growth inhibition. In summary, we have identified several novel anti-invasion mechanisms of YC-1 that could impact NPC, and possibly other cancers as well.

© 2009 Published by Elsevier Inc.

1. Introduction

Nasopharyngeal carcinoma (NPC) is a highly invasive and metastatic head and neck cancer prevalent in Southeast Asia with a high incidence rate of 15–50/100,000 persons/year (comparable to that of pancreatic cancer in the US) [1–3]. Over 50–70% of NPC patients present with advanced disease (stages IIb–IV) with lymph node invasion or metastasis at the time of diagnosis [4]. Recurrent NPC patients also have a high rate of distant metastasis up to 37% [5]. Although the underlying mechanism for its high metastatic characteristics is not fully understood, the search for anti-invasion or anti-metastatic drugs for advanced NPC is actively being pursued.

YC-1 [3-(5′-hydroxymethyl-2′-furyl)-1-benzylindazole] is a synthetic benzylindazole compound originally developed as an activator of guanylyl cyclase to inhibit platelet aggregation and vascular contraction [6]. Recent studies revealed that YC-1 has potent activity against tumor growth, angiogenesis, invasion and metastasis [7–9]. In multiple cancer models, YC-1 induced prominent suppression of tumor growth and prolongation of survival in tumor-bearing mice with established tumors [8–12]. The growth-inhibitory activity of YC-1 has been proposed to be mediated by: HIF-1α [9,12], STAT3 [13], MAPK [14], JNK [15], NF-κB [11], cell cycle-dependent pathway [14,16] and mitochondrial-dependent apoptosis pathway [10]. The recently described inhibitory activity of YC-1 on cellular invasion/metastasis in several *in vitro* and *in vivo* models of hepatoma, neuroblastoma and gastric and lung cancers [7,14] suggest the clinical potential of this agent for anti-invasion/anti-metastatic therapy. Studies are underway to identify the largely unknown anti-invasion or

Abbreviations: NPC, nasopharyngeal carcinoma; EBV, Epstein-Barr virus; RPPA, reverse phase protein array; EGF, epidermal growth factor; EGFR, epidermal growth factor receptor; MMP-2/-9, Matrix Metalloproteinases 2 and 9; ACC, acetyl-CoA carboxylase; AMPKα, AMP-activated protein kinase α; LMP1, latent membrane protein 1.

* Corresponding author at: Department of Clinical Oncology, Prince of Wales Hospital, Shatin, Hong Kong. Tel.: +852 2632 2099; fax: +852 2648 8842.
E-mail address: anthony@clo.cuhk.edu.hk (Anthony T.C. Chan).

[1] Denotes co-first authorship.

0006-2952/$ – see front matter © 2009 Published by Elsevier Inc.
doi:10.1016/j.bcp.2009.10.021

anti-metastatic mechanism(s) of YC-1, in addition to the potential involvement of HIF-1α and Matrix Metalloproteinases 2 and 9 (MMP-2/-9) [7,14]. A more detailed mechanistic understanding of its anti-invasion/anti-metastatic activity may facilitate its clinical application for aggressive cancers.

A quantitative functional proteomic platform, named reverse phase protein array (RPPA), has been recently employed for quantitative profiling of signaling protein expression in cancer [17]. With the capability to detect total, phospho-proteins, and translationally modified proteins in a highly quantitative manner with high sensitivity at femtogram level [18], this high-throughput multiplex functional proteomic approach can be used for signaling profiling, detection of disease marker expression, as well as for mechanistic studies of drug action [19–21]. Recently, we have employed RPPA for the identification of novel signaling changes induced by combined anti-EGFR and anti-GRPR therapies in head and neck cancer, which provide valuable insights for the mechanism of action of combination therapy [22].

In this study, we reported the anti-invasive, as well as anti-proliferative activities of YC-1 in NPC cell lines. We aimed at identifying novel anti-invasion mechanisms of YC-1 by RPPA scanning of signaling changes induced by YC-1 in NPC cells. Our study revealed for the first time that multiple invasion-related signaling proteins (β-catenin, caveolin, Src and EGFR), which were previously un-described signaling proteins altered by YC-1, were found to be down-modulated by YC-1 in NPC cells. We hypothesized that these invasion-related proteins (as identified to be downregulated by YC-1), may contribute to the anti-invasion mechanism of YC-1 in NPC cells. Rescue experiments demonstrated that overexpression of EGFR, activated Src or caveolin in NPC cells all resulted in reversal of YC-1-induced inhibition of cellular invasion, with EGFR and activated Src having additional effects on rescuing NPC cells from YC-1-induced growth inhibition. Using the NPC model, we have identified several novel anti-invasion mechanisms of YC-1.

2. Materials and methods

2.1. Reagents

YC-1 was purchased from AG Scientific, Inc., San Diego, CA, USA and dissolved in DMSO (Sigma–Aldrich, Saint Louis, MO, USA) at a stock concentration of 100 mM. Epidermal growth factor (EGF) was from Invitrogen (BioSource), Camarillo, CA, USA. Fetal bovine serum (FBS) was from Hyclone, Logan, UT, USA. Antibodies against phospho-p42/44 MAPK, phospho-STAT3(Y705), STAT3, cleaved PARP, mTOR, Src, phospho-ACC, caveolin, β-catenin, AMPKα, phospho-Chk1, phospho-Chk2, Chk1 and Chk2 were from Cell Signaling Technology, Danvers, MA, USA. Phospho-Src(Y418) antibody was from Invitrogen, Camarillo, CA, USA. Phospho-EGFR(Y1086) antibody was from Invitrogen (Zymed), Camarillo, CA, USA. EGFR monoclonal antibody was from BD Transduction Laboratories, San Jose, CA, USA. Actin antibody (JLA20) was from Calbiochem, EMD Biosciences, San Diego, CA, USA. Expression plasmids for β-catenin (pCl-neo β-catenin WT), activated Src (pLNCX chick srcY527F) and caveolin (Cav1-GFP) were from Addgene Inc., Cambridge, MA, USA. EGFR expression plasmid (pcDNA-HA-EGFR) was provided by Dr. Lan Ma (Fudan University, Shanghai, China).

2.2. Cell culture

Human nasopharyngeal carcinoma cell lines, HONE-1, HONE-1-LMP1, HK1, CNE-2 and C666-1 were cultured in complete RPMI (Hyclone, Logan, UT, USA) in a humidified incubator at 37 °C in 5% CO_2 as previously described [23]. HONE-1 and CNE-2 were of poorly differentiated NPC origin, while HK1 and C666-1 were derived from well-differentiated and undifferentiated NPC. HONE-1-LMP1 stably expresses the Epstein-Barr virus (EBV)-encoded latent membrane protein 1 (LMP1) (B95.8 variant) and was maintained in puromycin selection medium (400 ng/ml; Merck, Whitehouse Station, NJ, USA).

2.3. Cell viability assay

Cells (1.3×10^4 per well) were treated with various concentrations of YC-1 or vehicle control (DMSO) for 48 h. Cell viability was determined by MTT assay (MTT from Sigma–Aldrich, Saint Louis, MO, USA) as previously described [24]. Percentage of cell growth inhibition was calculated as $(OD_{vehicle} - OD_{drug})/OD_{vehicle} \times 100\%$. The IC_{50} value was the drug concentration at which 50% of maximal growth inhibition was observed.

2.4. Cell cycle analysis

After treatment with DMSO or YC-1 (700 nM) for 12 h, cells were fixed with ice-cold ethanol (70%) and subjected to cell cycle analysis as previously described [25].

2.5. Matrigel invasion assay

Invasiveness of NPC cells was evaluated using Matrigel-coated modified Boyden inserts (Becton Dickinson/Biocoat, BD Biosciences, Bedford, MA, USA) as previously described [23]. Briefly, HONE-1 (7×10^4) or CNE-2 cells (3.5×10^4) were seeded onto the upper chamber in serum-free medium. FBS (10%) or EGF (20 ng/ml) in serum-free medium was added to the bottom chamber in presence of DMSO or YC-1. Cells were incubated for 24 h at 37 °C. The invaded cells were fixed, stained, photographed (100× magnification) and counted (200× magnification) under the microscope. The average number of invaded cells/field of 6–10 fields was presented.

2.6. Transfection

HONE-1 cells (1.5×10^4 or 1.2×10^5) were seeded onto 24- or 6-well plates and incubated for 24 h. Cells were then transfected with 0.5 μg (24-well plate) or 4 μg (6-well plate) plasmids using Lipofectamine 2000 (Invitrogen, Carlsbad, CA, USA). For Matrigel invasion assay, two days after transfection, 7×10^4 transfectants were replated onto the upper chamber in serum-free medium. DMSO or YC-1 (700 nM) in complete medium was added to the bottom chamber. Cells were incubated for 24 h at 37 °C. For MTT assay, day 2 transfectants were treated with DMSO or YC-1 (1 and 5 μM) for 24 h, followed by MTT assay.

2.7. Western blotting

After drug treatment, protein lysates were collected for Western blot analysis as previously described [26]. Twenty-five micrograms of protein was used for SDS-PAGE. After primary and secondary antibody incubations, the signal was detected by Supersignal West Pico Chemiluminescent detection kit (Thermo Fisher Scientific, Waltham, MA, USA), followed by autoradiography.

2.8. RPPA sample preparation and slide printing

HONE-1 cells (1×10^6) were plated on 10 cm plates. After treatment, cells were collected by washing with ice-cold PBS, scrapping and centrifugation at 1500 rpm at 4 °C for 10 min. Cell pellets were resuspended in RPPA lysis buffer (1% Triton X-100,

50 mM HEPES (pH 7.4), 150 mM NaCl, 1.5 mM $MgCl_2$, 1 mM EGTA, 100 mM NaF, 10 mM NaPPi, 10% glycerol, 1 mM Na_3VO_4, and protease inhibitor (Roche Applied Science, Indianapolis, IN, USA)) and incubated on ice with occasional shaking for 20 min. The supernatant was collected by centrifugation at 14,000 rpm, 4 °C for 10 min and quantified by Bio-Rad protein assay (Bio-Rad laboratories, Hercules, CA, USA). Lysates were mixed with 4× SDS sample buffer (35% glycerol, 8% SDS, 0.25 mM Tris–HCl, pH 6.8) in final concentration of 1 μg/μl and denatured by boiling for 5 min. The samples were serially diluted with lysis buffer (1:2, 1:4, 1:8 and 1:16) and transferred to 384-well plates for array spotting. Lysates were arrayed onto nitrocellulose-coated FAST slides (Schleicher & Schuell BioScience Inc., Keene, NH, USA) using an Aushon Biosystems (Burlington, MA, USA) 2470 arrayer, which can create 1056 samples arrays per slide. Array spots of 1 nanoliter (nl) cell lysate were printed. For each slide, positive and negative control samples were included as well as multiple loading controls.

2.9. RPPA staining and data analysis

The RPPA procedures for antibody staining and signal detection were performed essentially as previously described [17]. Slides were probed with validated primary antibodies and the signal was amplified using the DakoCytomation-catalyzed system (Dako, Carpinteria, CA, USA). After staining, slides were scanned, analyzed and quantified using Microvigene software (VigeneTech Inc.,

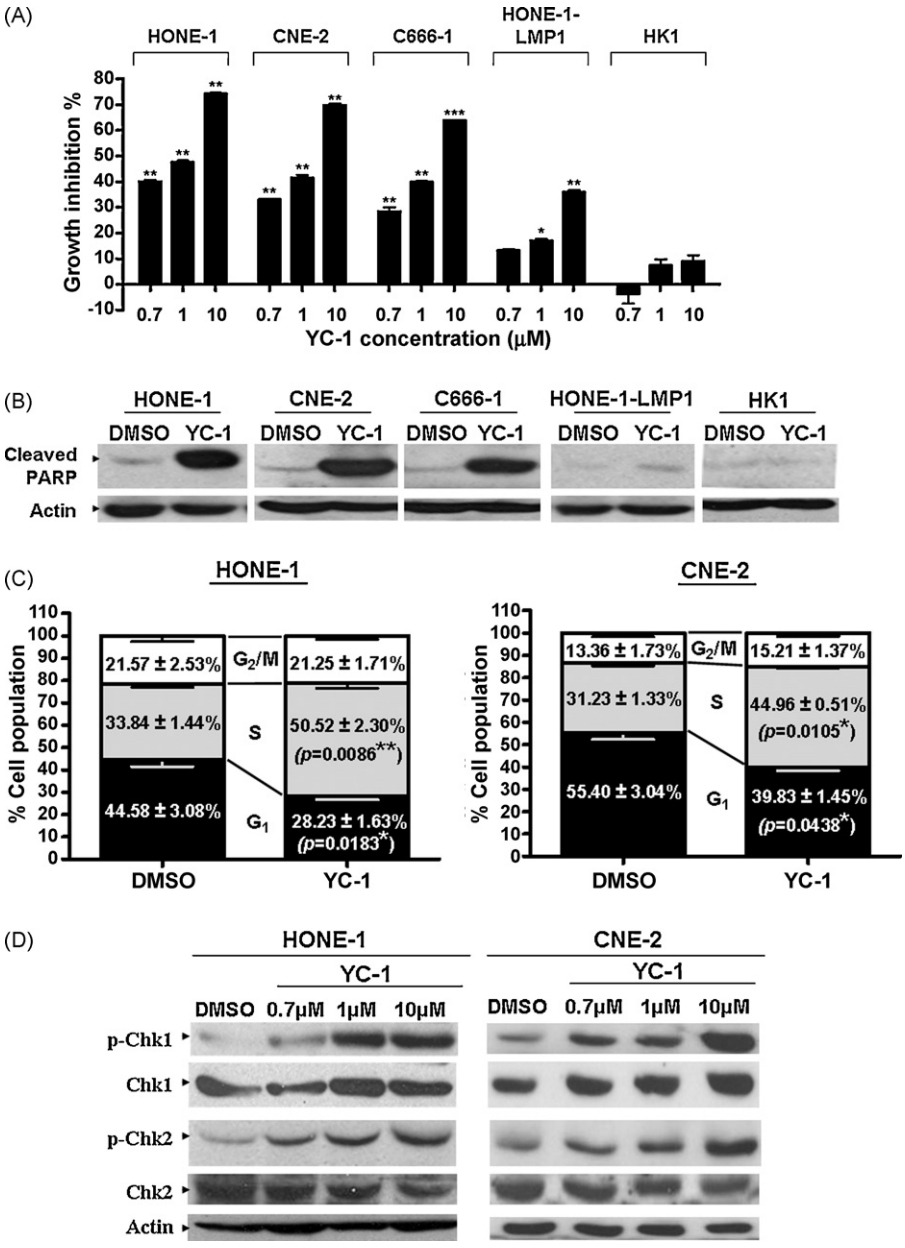

Fig. 1. YC-1 inhibited NPC cell growth associated with PARP cleavage, S-phase arrest and activation of Chk1/Chk2. (A) Dose-dependent growth inhibition of NPC cells by YC-1. The effect of YC-1 on NPC cell growth was assessed by MTT assay at 48 h (statistical significance of drug treatment vs. DMSO control: $p < 0.05^{*}$, $p < 0.01^{**}$, $p < 0.001^{***}$). (B) YC-1-induced growth inhibition was associated with PARP cleavage in YC-1-sensitive NPC cell lines. Western blot showing cleaved PARP expression in NPC cell lines upon YC-1 (10 μM) treatment for 24 h. (C) YC-1 induced S-phase cell cycle arrest. Cell cycle distribution of HONE-1 and CNE-2 cells treated with 700 nM YC-1 or DMSO for 12 h. Average percentage of cell population in different phases of the cell cycle was shown as mean ± SEM (n = 3, cumulative results from 3 independent experiments). Statistical significance of YC-1 treatment vs. DMSO control was indicated as $p < 0.01^{**}$ and $p < 0.05^{*}$. (D) YC-1 induced dose-dependent activation of Chk1 and Chk2. At 24 h, YC-1 induced dose-dependent phosphorylation of Chk1 and Chk2 in both HONE-1 and CNE-2 cells. Actin was used as a loading control. For all experiments, similar results were obtained in three independent experiments.

Carlisle, MA, USA) to generate serial dilution–signal intensity curves for each sample.

The RPPA spot signal intensity data were processed by the R package SuperCurve (version 1.01), available at "http://bioinformatics.mdanderson.org/OOMPA". A fitted curve (called "supercurve") was plotted with the signal intensities on the *Y*-axis and the relative log2 concentration of each protein on the *X*-axis using the non-parametric, monotone increasing B-spline model. The protein concentrations were derived from the supercurve for each sample lysate by curve-fitting and then normalized by median polish. Data were presented after normalization as normalized linear value.

2.10. Statistical analysis

All data were analyzed using PRISM4 Software (GraphPad Software, Inc., San Diego, CA, USA). Statistical analysis was performed using unpaired *t*-test with Welch's correction. Results were considered as statistically significant when $p < 0.05$.

3. Results

3.1. YC-1 inhibited NPC cell growth associated with PARP cleavage, S-phase arrest and activation of Chk1/Chk2

First, we examined the anti-tumor activity of YC-1 in a panel of 5 NPC cell lines (HONE-1, CNE-2, C666-1, HONE-1-LMP1 and HK1). As shown in Fig. 1A, all NPC cell lines exhibited a dose-dependent growth inhibition upon YC-1 treatment, except for HK1, which was rather insensitive to YC-1 even at 10 μM. At 10 μM, YC-1 induced a maximal growth inhibition of 74.1% in HONE-1, followed by 69.7% in CNE-2, 63.8% in C666-1, and 35.8% in HONE-1-LMP1 at 48 h, when compared with DMSO control. The relative sensitivity of NPC cell lines towards YC-1 was consistent with the observed induction of PARP cleavage (a hallmark for apoptosis) (Fig. 1B). YC-1-induced PARP cleavage was the strongest in HONE-1, CNE-2 and C666-1, followed by very moderate induction in HONE-1-LMP1 and no induction in HK1. The mechanism underlying the relative resistance of HK1 to YC-1 is unclear.

We then examined the effects of YC-1 on cell cycle progression of the two most sensitive NPC cell lines, HONE-1 and CNE-2. Both of these cell lines were originally derived from poorly differentiated NPC [27,28]. In both HONE-1 and CNE-2, YC-1 treatment (700 nM, the determined IC_{50} value of YC-1 at 48 h in HONE-1, Supplementary Fig. 1) resulted in S-phase arrest with concomitant reduction in G_1 population at 12 h, when compared to DMSO control (Fig. 1C). Our data showed that YC-1 induced an average increase of S-phase population by 16.68% (from 33.84 ± 1.44% to 50.52 ± 2.30%, cumulative results from 3 independent experiments, $n = 3$, $p = 0.0086$), and 13.73% (from 31.23 ± 1.33% to 44.96 ± 0.51%, cumulative results from 3 independent experiments, $n = 3$, $p = 0.0105$) in HONE-1 and CNE-2, respectively. The representative original cell cycle results by flow cytometry for both HONE-1 and CNE-2 cells are shown in Supplementary Fig. 2.

Since Chk1 and Chk2 are key regulators of S-phase checkpoint and their phosphorylation is known to prevent S-phase progression [29,30], we detected if the YC-1-induced S-phase arrest was associated Chk1 and Chk2 phosphorylation. As shown in Fig. 1D, YC-1-induced S-phase arrest was found to be associated

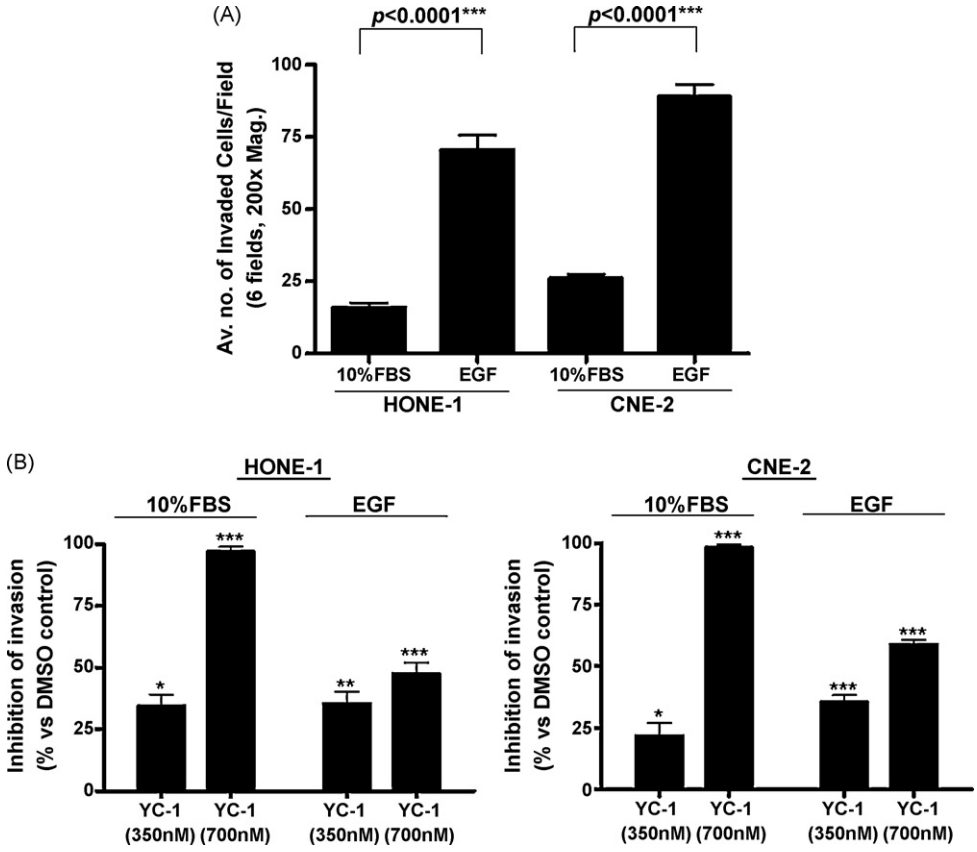

Fig. 2. YC-1 inhibited NPC cell invasion through the Matrigel. (A) EGF enhanced the cellular invasion activity of HONE-1 and CNE-2 cells. HONE-1 or CNE-2 cells were allowed to invade through the Matrigel chamber, with either serum (10% FBS) or EGF (20 ng/ml) as chemoattractants. The average number of invaded cells/field was presented as mean ± SEM ($n = 6$ fields, $p < 0.001^{***}$). (B) YC-1 inhibited FBS- and EGF-induced invasion of NPC cells. Invasion ability of HONE-1 and CNE-2 cells was assayed in the presence of YC-1 (or DMSO) in serum-free medium containing 10% FBS or EGF (20 ng/ml). Percentage of YC-1 induced-invasion inhibition was presented with reference to the respective DMSO control (statistical significance of YC-1 treatment vs. DMSO control: $p < 0.001^{***}$). Similar results were obtained in three independent experiments.

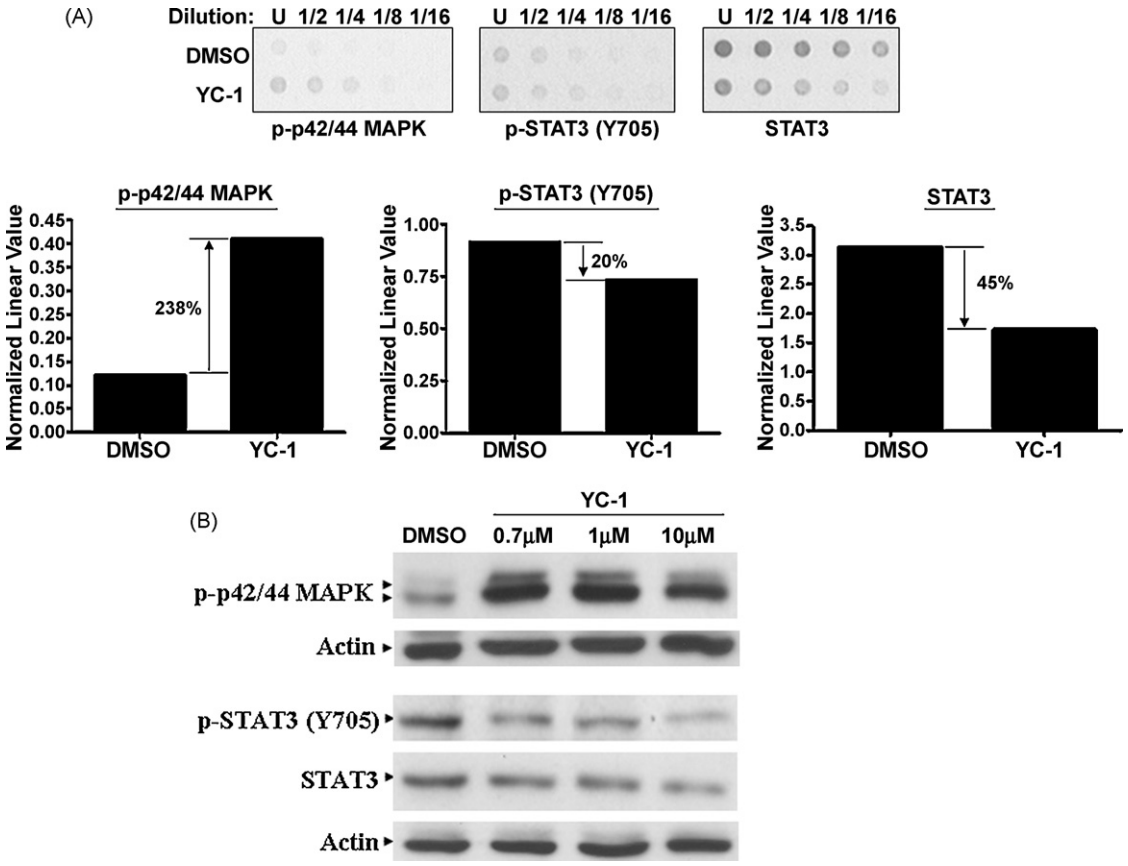

Fig. 3. RPPA results showing induction of phospho-p42/44 MAPK and downregulation of phospho-STAT3(Y705) and total STAT3 by YC-1 in HONE-1 cells. (A) Original RPPA spot intensities with quantitative graphical presentation for p-p42/44 MAPK, p-STAT3(Y705) and total STAT3 expression. Serial dilution (U: undiluted sample; 1/2, 1/4, 1/8, 1/16 dilution) of each sample was illustrated. HONE-1 cells were treated with 700 nM YC-1 or DMSO for 48 h. Protein lysates with serial dilution are arrayed onto nitrocellulose slides, and stained for p-p42/44 MAPK, p-STAT3(Y705) and total STAT3 (upper panel). The protein levels were quantified by Microvigene software and the normalized linear values were shown (lower panel). (B) Validation of RPPA results by Western blotting, showing a dose-dependent change in p-p42/44 MAPK, p-STAT3(Y705) and total STAT3 expression. HONE-1 cells were treated with the indicated concentrations of YC-1 or DMSO for 48 h. Cellular proteins were collected for Western Blotting. Actin was used as a loading control.

with dose-dependent phosphorylation of Chk1 and Chk2, which was consistent with previous findings in HEK293 cells [16].

3.2. YC-1 inhibited serum- and EGF-induced invasion of NPC cells

NPC cells are known to be intrinsically invasive. Therefore, in addition to evaluating its anti-proliferation activity, we also examined the potential anti-invasion activity of YC-1 on NPC cells. Both HONE-1 and CNE-2 cells were invasive (Fig. 2A). EGF further increased the invasiveness of HONE-1 and CNE-2 cells by 4.4-fold and 3.3-fold, respectively (from 16 ± 2 to 71 ± 5 cells/field for HONE-1; from 26 ± 1 to 89 ± 4 cells/field for CNE-2, $n = 6$, $p < 0.0001$) (Fig. 2A). YC-1, at nanomolar concentrations, was able to effectively reduce both serum-induced and EGF-induced cellular invasion through the Matrigel in a dose-dependent manner at 24 h. At 700 nM, YC-1 almost completely abrogated the serum-induced invasion of HONE-1 and CNE-2 (with 96.9% and 98.1% inhibition, respectively) (Fig. 2B). Even in the presence of the strong invasion-inducer, EGF, YC-1 at 700 nM was able to inhibit EGF-induced invasion by 47.4% and 58.7% in HONE-1 and CNE-2, respectively (Fig. 2B).

3.3. Reverse phase protein array identifies novel signaling changes by YC-1 treatment

The potent anti-invasion activity of YC-1, together with its anti-proliferative effect in NPC cell lines, indicates its potential use as an anti-invasion agent for NPC. The mechanisms underlying YC-1's anti-invasion activity in NPC is largely unknown. Although multiple signaling pathways have been proposed to contribute to YC-1's anti-proliferative activity in several human cancers (e.g. HIF-1α [9,12], STAT3 [13], MAPK [14], JNK [15], NF-κB [11], cell cycle-dependent pathway [14,16] and mitochondrial-dependent apoptosis pathway [10]), little is known about the mechanisms

Table 1
Quantitative results of RPPA profiling showing invasion- or proliferation-related signaling proteins downregulated by YC-1. Invasion-related signaling proteins (A) and proliferation-related signaling proteins (B) downregulated by YC-1 (700 nM) in HONE-1 cells at 48 h were indicated. Percentage change versus DMSO control was shown.

Proteins	% Change vs. DMSO
A: Invasion-related signaling proteins downregulated by YC-1	
β-catenin	50.3%
Caveolin	49.3%
Src	37.2%
EGFR	20.6%
B: Proliferation-related signaling proteins downregulated by YC-1	
STAT3	44.8%
AMPKα	27.5%
ACC (S79)	26.6%
HER-2	26.0%
mTOR	22.5%
p-STAT3 (Y705)	19.8%

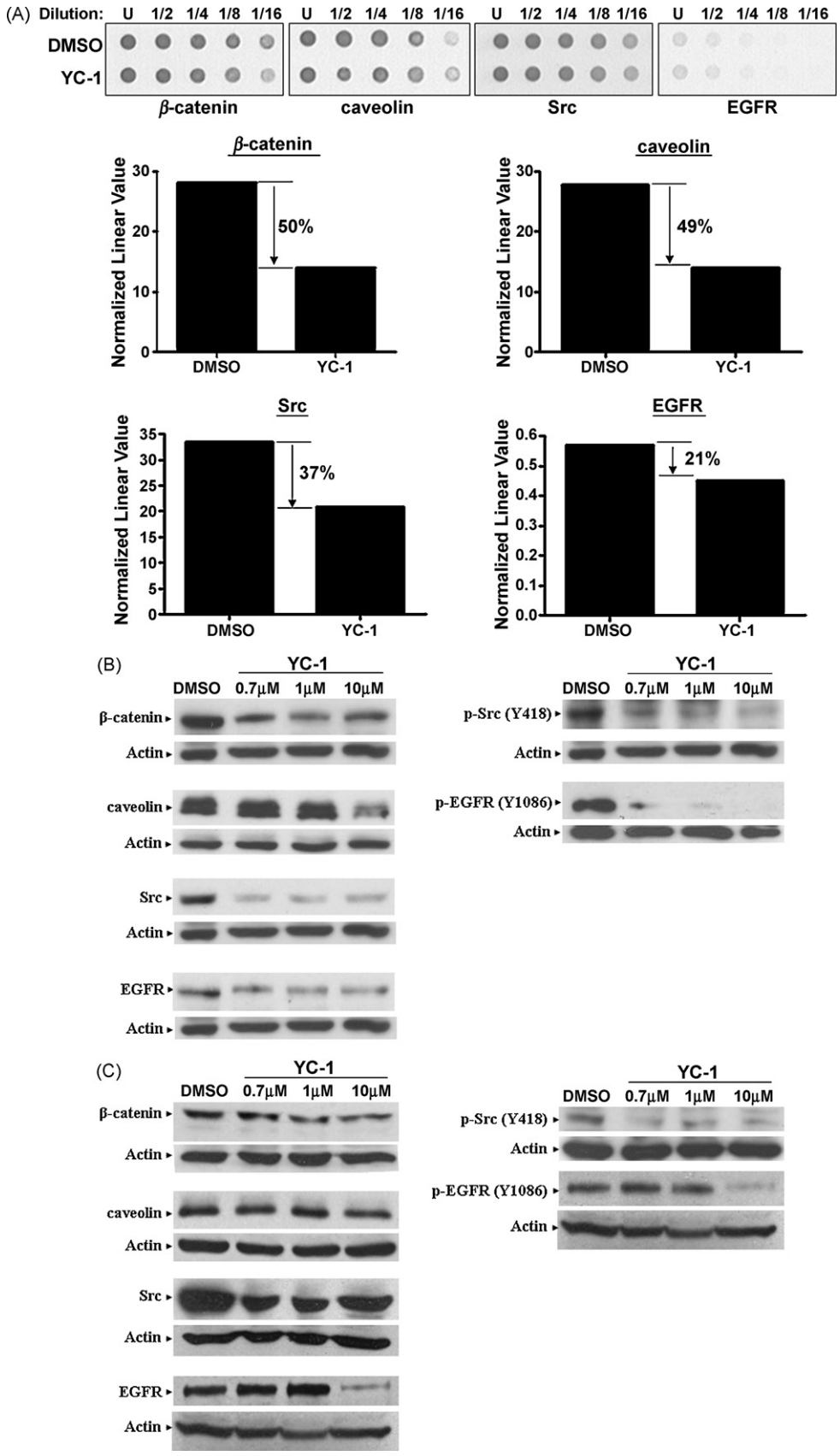

Fig. 4. RPPA revealed downregulation of several invasion-related proteins by YC-1 in HONE-1 cells. (A) Original RPPA spot intensities (upper panel) with quantitative graphical presentation (lower panel) for β-catenin, caveolin, Src and EGFR. HONE-1 cells were treated with 700 nM YC-1 or DMSO for 48 h and normalized linear values were shown. (B) Validation of RPPA results by Western blotting, showing a dose-dependent change in the expression levels of β-catenin, caveolin, Src and EGFR in HONE-1 cells at 48 h (left panel). Western blot analysis indicated that the phospho-forms of Src and EGFR were also downregulated by YC-1 at 48 h (right panel). Actin was used as a loading control. (C) Downregulation of invasion-related signaling proteins by YC-1 in HONE-1 as early as 24 h. Western blot analysis indicated that dose-dependent inhibition of Src, phospho-Src(Y418), β-catenin, EGFR, phospho-EGFR(Y1086) and caveolin expression by YC-1.

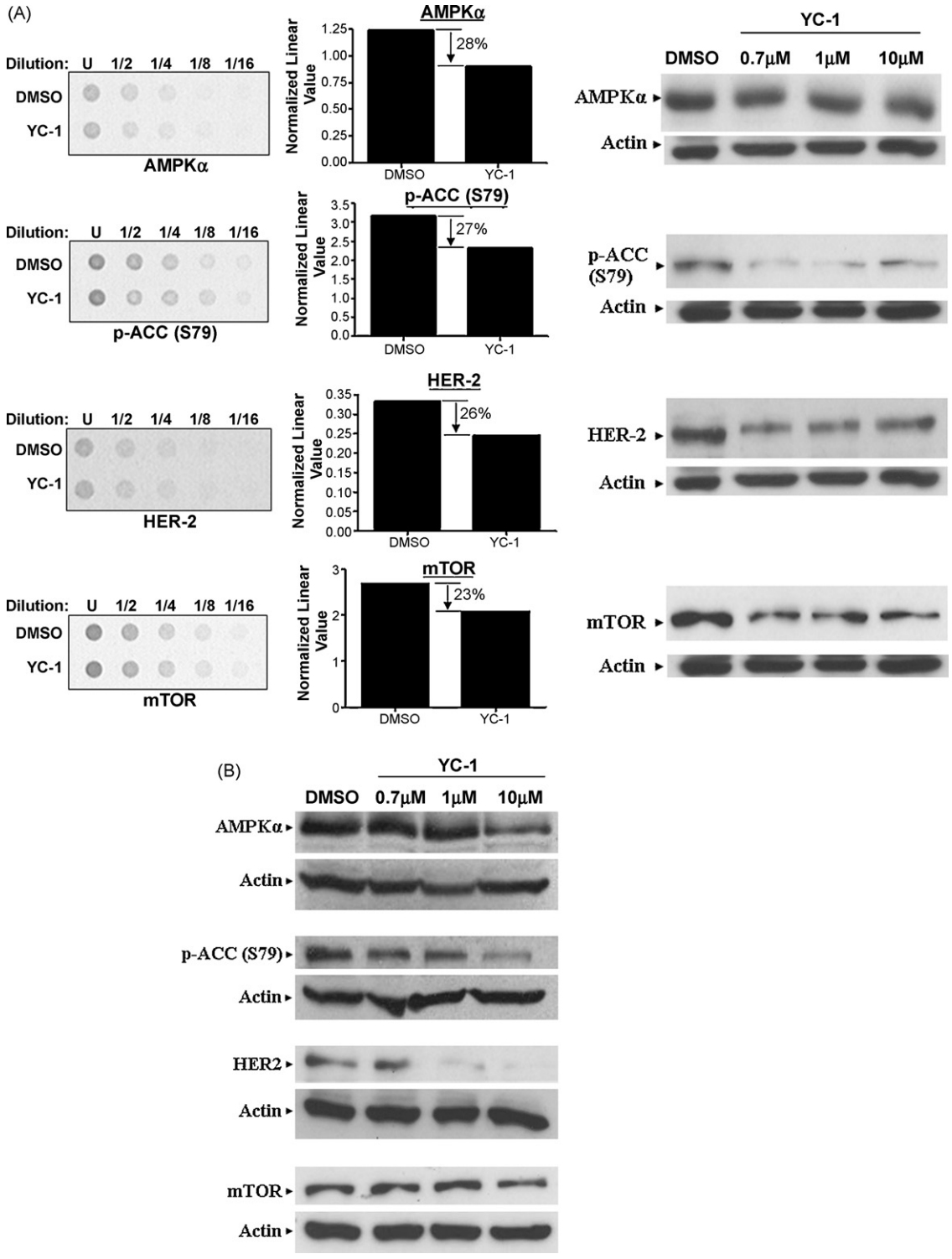

Fig. 5. RPPA revealed downregulation of several proliferation-related proteins by YC-1 in HONE-1 cells. (A) RPPA revealed several previously un-described proliferation-related proteins (AMPKα, p-ACC, HER-2 and mTOR) were downregulated by YC-1 in HONE-1 cells at 48 h. The original RPPA spot intensities (left panel), graphical presentation of the quantitative data (middle panel) and Western blot validation (right panel) were shown. (B) Downregulation of proliferation-related signaling proteins by YC-1 in HONE-1 as early as 24 h. Western blot analysis indicated that dose-dependent inhibition of AMPKα, p-ACC, HER-2 and mTOR expression by YC-1. Actin was used as a loading control.

underlying its anti-invasion activity besides the potential involvement of HIF-1α and MMP2/9 [7,14]. Therefore, we employed a quantitative proteomic approach, the reverse phase protein array, to elucidate the potential anti-invasion mechanisms of YC-1 in NPC cells.

Using specific antibodies recognizing the phosphorylated and total form of various signaling proteins, RPPA can multiplex and quantify a large array of signaling proteins with high reproducibility [18]. A quantitative comparison of expression profiles of 70 signaling proteins was performed for HONE-1 cells (the most YC-1-sensitive cell line) treated with DMSO or YC-1 (700 nM) for 48 h with 70 optimized antibodies as previously described [21]. For quantification purpose, cell lysates with serial dilution were analyzed by RPPA [31] and the amount of each signaling protein

was determined using the Microvigene software as previously described [19,22].

The RPPA analysis demonstrated that 14 out of 70 signaling proteins were upregulated and 23/70 were downregulated by YC-1 at 48 h (with changes ≥20% vs. DMSO control; Supplementary Table 1). Among the list, several signaling proteins previously known to be involved in the anti-tumor activity of YC-1 were also found to be altered in NPC cells and were validated by Western blotting with a dose-dependent trend (Fig. 3) [13,32]. These include: YC-1-induced upregulation of phospho-p42/44 MAPK (by 238%) and downregulation of phospho-STAT3(Y705) (by 20%), when compared to DMSO control. Our RPPA result showed that down-modulation of phospho-STAT3(Y705) was actually accompanied by reduction of total STAT3 protein as well (by 45%), which has not been observed in previous study [13] (Fig. 3).

In order to analyze which signaling pathways were concordantly altered by YC-1 treatment, the identified signaling changes were grouped according to the respective known pathways or biological functions. This pathway analysis of the RPPA results showed that YC-1 exerted major effects on several important signaling pathways, including the MAPK pathway, cell cycle-related pathways, PI3K pathway, tyrosine kinase pathway, STAT3 pathway and metabolism-related pathways (Supplementary Table 1). Interestingly, quantitative analysis of invasion-related proteins revealed specific downregulation of β-catenin (by 50%), caveolin (by 49%), total Src (by 37%) and EGFR (by 21%) by YC-1 (700 nM) in HONE-1 cells at 48 h, when compared to DMSO control (Table 1A, Fig. 4A). These YC-1-induced changes in invasion-related proteins have not been previously reported. A dose-dependent reduction of all these identified invasion-related proteins by YC-1 at 48 h was confirmed and validated by Western blotting (Fig. 4B, left panel). As both Src and EGFR are activated by phosphorylation, we anticipated the observed down-modulation of total Src and EGFR to be accompanied by reduction of their phosphorylated forms, which was confirmed by Western blotting (Fig. 4B, right panel). Indeed, these changes were consistently observed by Western blot analysis even at 24 h upon YC-1 treatment (Fig. 4C). In addition, several other proliferation-related proteins were also down-regulated by YC-1, which included AMPKα, p-ACC, HER-2 and mTOR (Table 1B). Similarly, these RPPA findings were all confirmed and validated by Western blotting (Fig. 5A and B).

3.4. Inhibitory effects of YC-1 on NPC cell invasion were reversed by overexpression of EGFR, activated Src or caveolin

EGFR, β-catenin, Src and caveolin are known to be important players in cell invasion and metastasis [33–36]. RPPA analyses revealed for the first time that expression of these invasion-related proteins were downregulated by YC-1, implicating their potential involvement in the anti-invasion activity of YC-1 in NPC cells. This was further examined by rescue experiments to determine if overexpression of these proteins could reverse the inhibitory effects of YC-1 on NPC cell invasion. As shown in Fig. 6A, YC-1 (700 nM) significantly inhibited cellular invasion of vector-transfected HONE-1 cells at 24 h. However, this YC-1-induced inhibition of NPC cell invasion was rescued by overexpression of EGFR, activated Src (Src Y527F) or caveolin ($p < 0.0001^{***}$) (Fig. 6A), whereas overexpression of β-catenin did not exert any significant effect on the anti-invasion activity of YC-1 (Fig. 6A). We also examined if these invasion-related proteins also mediated YC-1-induced growth inhibition of NPC cells. As shown in Fig. 6B, overexpression of either EGFR or activated Src (Src Y527F) was able to reduce YC-1-mediated growth inhibition of NPC cells. Our results demonstrated that only EGFR and activated Src had additional effects on rescuing NPC cells from YC-1-induced growth inhibition (Fig. 6B), but not β-catenin and caveolin (data not shown). Thus, while EGFR and Src participate in both the anti-proliferative and anti-invasive activity of YC-1, caveolin is only involved in its anti-invasive activity.

In summary, using RPPA, we demonstrated for the first time that multiple invasion-related signaling proteins were down-regulated by YC-1 (including β-catenin, caveolin, Src, and EGFR), in addition to several proliferation-related proteins. More importantly, we identified novel anti-invasion mechanisms of YC-1 in NPC cells via down-modulation of EGFR, Src and caveolin.

4. Discussion

In the present study, we showed that YC-1 effectively inhibited NPC cell invasion and cell proliferation at nM range. Growth inhibition of NPC cells was associated with PARP cleavage and cell cycle arrest at S-phase. Functional proteomic analysis by reverse phase protein array identified for the first time that multiple invasion-related signaling proteins, including β-catenin, caveolin, Src and EGFR, were downregulated by YC-1 in cancer cells, indicating that this high throughput functional proteomics approach has the ability to help define the mechanism of action of active drugs. Finally, overexpression of EGFR, activated Src or caveolin, but not β-catenin reversed YC-1-induced inhibition of NPC cell invasion, demonstrating these newly identified signaling proteins altered by YC-1 treatment to be novel mediators of YC-1's anti-invasion activity in NPC. Thus, RPPA profiling of signaling proteins allowed us to identify several novel anti-invasion mechanisms of YC-1 that could impact NPC, and possibly other cancers as well.

In preclinical models, YC-1 exhibits anti-invasion or anti-metastatic activities in various human cancer cell lines, including hepatoma, neuroblastoma and gastric carcinoma. Using *in vivo* models of liver and lung cancers, Shin et al. showed that YC-1 was able to significantly reduce cancer cell metastasis or invasion to liver and lung, respectively [7]. Compared to the reported anti-proliferation mechanisms of YC-1 [9–16], the anti-invasion/anti-metastasis mechanisms of YC-1 remain largely unknown, excepted for the involvement of HIF-1α and MMP-2/-9 in hepatoma and non-small cell lung cancer cells [7,14]. As reported by Shin et al., YC-1 inhibited cell invasive migration more effectively than HIF-1α siRNA, suggesting the existence of addition mechanisms of anti-invasion of YC-1 in addition to HIF-1α inhibition [7]. In this study, we demonstrated that a functional proteomic platform, RPPA, could provide quantitative analysis of an array of important signaling proteins altered by this promising anti-cancer agent. The proteomic profile was useful in identifying novel signaling proteins altered by YC-1, providing information on the mechanism of action of this drug.

Using RPPA, several previously unidentified invasion-related proteins were found to be downregulated (>20%) by YC-1 in NPC cells (e.g. β-catenin, caveolin, Src and EGFR). Some of these newly identified signaling proteins altered by YC-1 are well-known key regulators of cancer cell invasion and metastasis, such as EGFR, Src and β-catenin [33–35]. Of these, EGFR and β-catenin are known to be overexpressed in NPC. Overexpression of EGFR correlates with shorter overall survival and time to progression in NPC patients, while β-catenin expression was not correlated with clinical outcome [37,38]. Recently, caveolin has been implicated in cancer metastasis and is found to be up-regulated in a various metastatic cancers including hepatocellular carcinoma [39], esophageal squamous cell carcinoma [40], renal cell carcinoma [41] and prostate cancer [42]. Studies revealed that it plays an important role in regulating cell migration, motility and cell–cell (matrix) adhesion [36]. A recent study by Du et al. demonstrated that caveolin was overexpressed in NPC biopsies, which correlated significantly with metastasis, poor survival and local recurrence

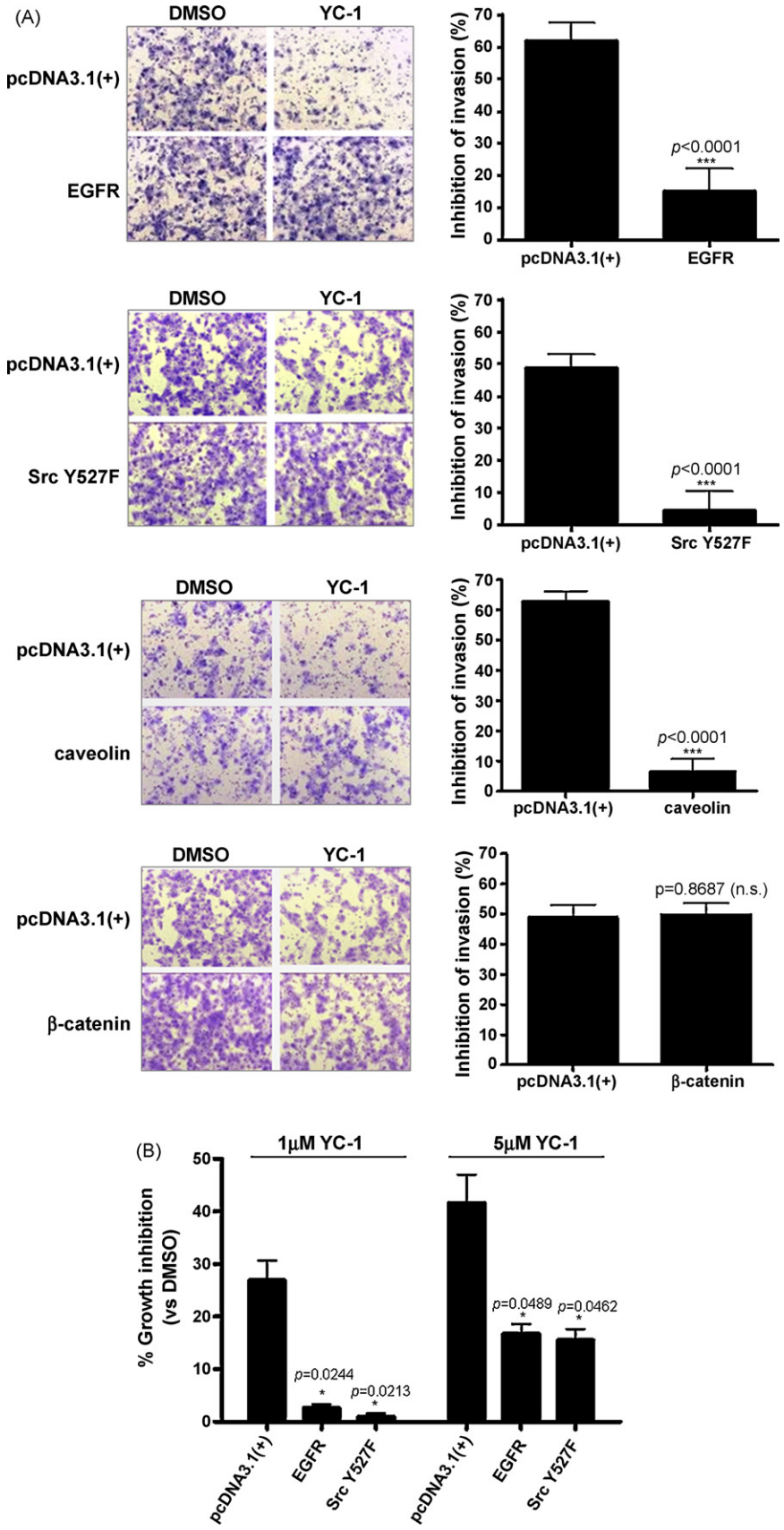

Fig. 6. (A) Inhibitory effects of YC-1 on NPC invasion were reversed by overexpression of EGFR, activated Src or caveolin. HONE-1 cells were transfected with 4 μg of pcDNA3.1(+) vector control, pcDNA-HA-EGFR, pLNCX chick src (Y527F), caveolin-GFP or pCI-neo β-catenin WT plasmid. For Matrigel invasion assay, two days after transfection, cells were replated into Matrigel invasion chamber and incubated for 24 h in the presence of DMSO or YC-1 (700 nM), respectively. Results were photographed at 100× (left panel). Percentage of inhibition of invasion induced by YC-1 was shown with reference to the respective DMSO control in each group as mean ± SEM (n = 10 fields) (right panel). (B) Overexpression of EGFR or activated Src also reversed the NPC growth inhibitory effect of YC-1. Day 2 transfectants were treated with 1 μM or 5 μM of YC-1 for

[43]. Caveolin was also found to be up-regulated in NPC cell lines (CNE1, CNE2 and C666-1) when compared with normal nasopharyngeal epithelial cells. Du et al. indicated that caveolin promoted NPC cell invasion and metastasis, which was consistent with our finding [43].

In this study, we found that EGFR, activated Src and caveolin are mediators of YC-1's anti-invasion activity in NPC cells. Since these signaling proteins are widely overexpressed and responsible for invasion or metastasis in many other human cancers, it may implicate the potential of YC-1 in inhibiting cancer cell invasion or metastasis of other cancers via targeted inhibition of EGFR, Src and caveolin. This may warrant further investigation in other cancers.

Our study demonstrated that YC-1-inhibited NPC cell growth was associated with apoptosis, as well as S-phase arrest with Chk1/2 phosphorylation. Chk1 and Chk2 are two important sensors of DNA damage. They are known to be phosphorylated upon DNA damage, which then inhibit the initiation of DNA replication and lead to a halt in S-phase of the cell cycle [30]. It is possible that the observed YC-1-mediated S-phase arrest in NPC cells is due to Chk1/2 phosphorylation and subsequent inhibition of DNA replication. YC-1 has been demonstrated to inhibit DNA synthesis in human vascular endothelial cells [44] and rat mesangial cells [45]. This is further supported by Yeo et al.'s finding that specific down-regulation of Chk1/2 by siRNA rescued YC-1-induced S-phase arrest in HEK293 cells [16].

Besides the involvement of Chk1/2, multiple anti-proliferation mechanisms of YC-1 have been previously described in various cancer systems including: downregulation of HIF-1α [9,12], activation of p44/42 MAPK [14] and JNK [15], inhibition of NF-κB activation [11] and phospho-STAT3 [13], induction of mitochondrial-dependent apoptosis pathway [14], as well as alteration of several cell cycle regulators, such as p21, p27, p16, cyclin D1, CDK2, cdc25A [14]. In this study using RPPA, we identified several previously un-described proliferation and metabolism-related signaling proteins altered by YC-1 in NPC (Table 1B). These include: AMPKα, p-ACC, HER-2, and mTOR. We also demonstrated activation of p44/42 MAPK and downregulation of phospho-STAT3 by YC-1 (Fig. 3B), which was consistent with previous findings [13,16,32]. Whether these new targets of YC-1 (AMPKα, p-ACC, HER-2 and mTOR) are responsible for YC-1's antitumor activity remain to be further investigated.

Of note was the finding that in the YC-1-insensitive cell line, HK1, addition of YC-1 (up to 10 μM for 48 h) did not induce any significant changes in the levels of EGFR, p-EGFR, Src, p-Src, caveolin, β-catenin (the invasion-related proteins), nor p-p44/42 MAPK, STAT3, p-STAT3, AMPKα, p-ACC, HER-2, and mTOR (the proliferation-related proteins) (Supplementary Fig. 3). These results agreed with our RPPA finding on the mechanistic involvement of these signaling cascades in the antitumor action of YC-1 in YC-1-sensitive cells, but not in YC-1-insensitive NPC cells. Our results showed that overexpression of EGFR or activated Src partially reduced YC-1-mediated growth inhibition, indicating their potential involvement in the anti-proliferative mechanism of YC-1. This may also explain why the HK1 cell line, which harbors EGFR gene amplification [46,47] together with elevated expression of EGFR, as well as Src (when compared with HONE-1) was relatively insensitive to YC-1 (Supplementary Fig. 4A). Moreover, in HONE-1-LMP1 cells (which showed moderate sensitivity to YC-1), the protein expression of EGFR and Src were also moderately upregulated when compared to HONE-1 (Supplementary Fig. 4B), which may partially explain the moderate sensitivity of this cell line to YC-1. In fact, LMP1 has been previously shown to induce EGFR expression [48]. Interestingly, although caveolin was found to be downregulated by YC-1 in HONE-1 cells (by RPPA) but not involved in the anti-proliferation action of YC-1, both HK1 and HONE-1-LMP1 expressed higher basal levels of this protein (vs. HONE-1) (Supplementary Fig. 4A and B).

Using RPPA, we have successfully identified several novel anti-invasion mechanisms of YC-1 in NPC. Although RPPA has been shown to be useful to detect quantitative changes in key signaling molecules, there are still practical limitations to be overcome in the future. Due to the stringent requirement of specific and high quality antibodies for RPPA (including antibodies for the total and/or phosphorylated protein or other modifications), the current pre-validated antibody set only allows the detection of limited number of very common and important signaling molecules. In the current study, only 70 well-validated signaling proteins were covered in the RPPA analysis. It is likely that some other signaling molecules, which may also contribute to anti-tumor action of YC-1, have not been evaluated by our RPPA platform at the moment. Hopefully, this practical limitation of RPPA can be resolved in the near future with concerted efforts for RPPA antibody validation to expand the potential number of specific and high quality antibodies that can be used for this highly quantitative proteomic platform.

In conclusion, YC-1 exhibits potent anti-invasion and anti-proliferation activities in NPC cell lines. Using RPPA, we identified novel YC-1-induced molecular changes and also identified novel anti-invasion mechanisms of YC-1, namely downregulation of EGFR, activated Src and caveolin in NPC. These identified mechanisms may also underlie the anti-invasive/anti-metastatic activity of YC-1 in other cancers. Results from our study may have important implications for the use of this promising anti-cancer agent for the treatment of NPC invasion or metastasis, which will warrant further investigation in metastatic models of NPC.

Conflict of interest

Authors have no financial/commercial conflicts of interest regarding the study.

Acknowledgements

Thanks for the kind provision of pcDNA-HA-EGFR by Dr. Lan Ma (Fudan University, China). This study was supported by Research Grant Council, Hong Kong Government (CUHK4442/06M, to ATC Chan and EP Hui). Result of this study was presented in parts at AACR conferences: Molecular Targeting and Cancer Therapeutics, USA, 2007; Infection and Cancer: Biology, Therapeutics and Prevention, Hong Kong, 2008.

Appendix A. Supplementary data

Supplementary data associated with this article can be found, in the online version, at doi:10.1016/j.bcp.2009.10.021.

References

[1] Chan AT, Teo PM, Johnson PJ. Nasopharyngeal carcinoma. Ann Oncol 2002;13:1007–15.
[2] Spano JP, Busson P, Atlan D, Bourhis J, Pignon JP, Esteban C, et al. Nasopharyngeal carcinomas: an update. Eur J Cancer 2003;39:2121–35.
[3] Anderson KE, Mack TM, Silverman DT. Cancer of the pancreas. In: Schottenfeld D, Fraumeni Jr JF, editors. Cancer epidemiology and prevention. New York: Oxford University Press; 2006. p. 721–62.
[4] Skinner DW, Van Hasselt CA, Tsao SY. Nasopharyngeal carcinoma: modes of presentation. Ann Otol Rhinol Laryngol 1991;100:544–51.

24 h. MTT assay was performed. Percentage of growth inhibition was shown with reference to their respective DMSO control in each group. Statistical difference between the pcDNA3.1(+) and the EGFR or activated Src (SrcY527F) transfected groups was indicated. Similar results were obtained in three independent experiments.

[5] Isobe K, Ito H, Shigematsu N, Kawada T, Yasuda S, Hara R, et al. Advanced nasopharyngeal carcinoma treated with chemotherapy and radiotherapy: distant metastasis and local recurrence. Int J Oncol 1998;12:1183–7.
[6] Ko FN, Wu CC, Kuo SC, Lee FY, Teng CM. YC-1, a novel activator of platelet guanylate cyclase. Blood 1994;84:4226–33.
[7] Shin DH, Kim JH, Jung YJ, Kim KE, Jeong JM, Chun YS, et al. Preclinical evaluation of YC-1, a HIF inhibitor, for the prevention of tumor spreading. Cancer Lett 2007;255:107–16.
[8] Pan SL, Guh JH, Peng CY, Wang SW, Chang YL, Cheng FC, et al. YC-1 [3-(5′-hydroxymethyl-2γ-furyl)-1-benzyl indazole] inhibits endothelial cell functions induced by angiogenic factors in vitro and angiogenesis in vivo models. J Pharmacol Exp Ther 2005;314:35–42.
[9] Chun YS, Yeo EJ, Park JW. Versatile pharmacological actions of YC-1: anti-platelet to anticancer. Cancer Lett 2004;207:1–7.
[10] Chung JG, Yang JS, Huang LJ, Lee FY, Teng CM, Tsai SC, et al. Proteomic approach to studying the cytotoxicity of YC-1 on U937 leukemia cells and antileukemia activity in orthotopic model of leukemia mice. Proteomics 2007;7:3305–17.
[11] Huang YT, Pan SL, Guh JH, Chang YL, Lee FY, Kuo SC, et al. YC-1 suppresses constitutive nuclear factor-kappaB activation and induces apoptosis in human prostate cancer cells. Mol Cancer Ther 2005;4:1628–35.
[12] Yeo EJ, Chun YS, Cho YS, Kim J, Lee JC, Kim MS, et al. YC-1: a potential anticancer drug targeting hypoxia-inducible factor 1. J Natl Cancer Inst 2003;95:516–25.
[13] Lau CK, Yang ZF, Lam SP, Lam CT, Ngai P, Tam KH, et al. Inhibition of Stat3 activity by YC-1 enhances chemo-sensitivity in hepatocellular carcinoma. Cancer Biol Ther 2007;6:1900–7.
[14] Chen CJ, Hsu MH, Huang LJ, Yamori T, Chung JG, Lee FY, et al. Anticancer mechanisms of YC-1 in human lung cancer cell line, NCI-H226. Biochem Pharmacol 2008;75:360–8.
[15] Wu SY, Pan SL, Chen TH, Liao CH, Huang DY, Guh JH, et al. YC-1 induces apoptosis of human renal carcinoma A498 cells in vitro and in vivo through activation of the JNK pathway. Br J Pharmacol 2008;155:505–13.
[16] Yeo EJ, Ryu JH, Chun YS, Cho YS, Jang IJ, Cho H, et al. YC-1 induces S cell cycle arrest and apoptosis by activating checkpoint kinases. Cancer Res 2006;66:6345–52.
[17] Tibes R, Qiu Y, Lu Y, Hennessy B, Andreeff M, Mills GB, et al. Reverse phase protein array: validation of a novel proteomic technology and utility for analysis of primary leukemia specimens and hematopoietic stem cells. Mol Cancer Ther 2006;5:2512–21.
[18] Sheehan KM, Calvert VS, Kay EW, Lu Y, Fishman D, Espina V, et al. Use of reverse phase protein microarrays and reference standard development for molecular network analysis of metastatic ovarian carcinoma. Mol Cell Proteomics 2005;4:346–55.
[19] Grote T, Siwak DR, Fritsche HA, Joy C, Mills GB, Simeone D, et al. Validation of reverse phase protein array for practical screening of potential biomarkers in serum and plasma: accurate detection of CA19-9 levels in pancreatic cancer. Proteomics 2008;8:3051–60.
[20] Charboneau L, Tory H, Chen T, Winters M, Petricoin EF, Liotta LA, et al. Utility of reverse phase protein arrays: applications to signalling pathways and human body arrays. Brief Funct Genomic Proteomic 2002;1:305–15.
[21] Kim WY, Chang DJ, Hennessy B, Kang HJ, Yoo J, Han SH, et al. A novel derivative of the natural agent deguelin for cancer chemoprevention and therapy. Cancer Prev Res (Phila PA) 2008;1:577–87.
[22] Zhang Q, Bhola NE, Lui VW, Siwak DR, Thomas SM, Gubish CT, et al. Antitumor mechanisms of combined gastrin-releasing peptide receptor and epidermal growth factor receptor targeting in head and neck cancer. Mol Cancer Ther 2007;6:1414–24.
[23] Lui VW, Wong EY, Ho Y, Hong B, Wong SC, Tao Q, et al. STAT3 activation contributes directly to Epstein-Barr virus-mediated invasiveness of nasopharyngeal cancer cells in vitro. Int J Cancer 2009;125:1884–93.
[24] Lui VW, Boehm AL, Koppikar P, Leeman RJ, Johnson D, Ogagan M, et al. Antiproliferative mechanisms of a transcription factor decoy targeting signal transducer and activator of transcription (STAT) 3: the role of STAT1. Mol Pharmacol 2007;71:1435–43.
[25] Wong JH, Lui VW, Umezawa K, Ho Y, Wong EY, Ng MH, et al. A small molecule inhibitor of NF-kappaB, dehydroxymethylepoxyquinomicin (DHMEQ), suppresses growth and invasion of nasopharyngeal carcinoma (NPC) cells. Cancer Lett; in press.
[26] Lui VW, Thomas SM, Zhang Q, Wentzel AL, Siegfried JM, Li JY, et al. Mitogenic effects of gastrin-releasing peptide in head and neck squamous cancer cells are mediated by activation of the epidermal growth factor receptor. Oncogene 2003;22:6183–93.
[27] Glaser R, Zhang HY, Yao KT, Zhu HC, Wang FX, Li GY, et al. Two epithelial tumor cell lines (HNE-1 and HONE-1) latently infected with Epstein-Barr virus that were derived from nasopharyngeal carcinomas. Proc Natl Acad Sci USA 1989;86:9524–8.
[28] Sizhong Z, Xiukung G, Yi Z. Cytogenetic studies on an epithelial cell line derived from poorly differentiated nasopharyngeal carcinoma. Int J Cancer 1983;31:587–90.
[29] Sancar A, Lindsey-Boltz LA, Unsal-Kacmaz K, Linn S. Molecular mechanisms of mammalian DNA repair and the DNA damage checkpoints. Annu Rev Biochem 2004;73:39–85.
[30] Bartek J, Lukas C, Lukas J. Checking on DNA damage in S phase. Nat Rev Mol Cell Biol 2004;5:792–804.
[31] Nishizuka S, Charboneau L, Young L, Major S, Reinhold WC, Waltham M, et al. Proteomic profiling of the NCI-60 cancer cell lines using new high-density reverse-phase lysate microarrays. Proc Natl Acad Sci USA 2003;100:14229–34.
[32] Chang MS, Lee WS, Teng CM, Lee HM, Sheu JR, Hsiao G, et al. YC-1 increases cyclo-oxygenase-2 expression through protein kinase G- and p44/42 mitogen-activated protein kinase-dependent pathways in A549 cells. Br J Pharmacol 2002;136:558–67.
[33] Kalyankrishna S, Grandis JR. Epidermal growth factor receptor biology in head and neck cancer. J Clin Oncol 2006;24:2666–72.
[34] Iiizumi M, Liu W, Pai SK, Furuta E, Watabe K. Drug development against metastasis-related genes and their pathways: a rationale for cancer therapy. Biochim Biophys Acta 2008;1786:87–104.
[35] Summy JM, Gallick GE. Src family kinases in tumor progression and metastasis. Cancer Metastasis Rev 2003;22:337–58.
[36] van Golen KL. Is caveolin-1 a viable therapeutic target to reduce cancer metastasis? Expert Opin Ther Targets 2006;10:709–21.
[37] Ma BB, Poon TC, To KF, Zee B, Mo FK, Chan CM, et al. Prognostic significance of tumor angiogenesis, Ki 67, p53 oncoprotein, epidermal growth factor receptor and HER2 receptor protein expression in undifferentiated nasopharyngeal carcinoma—a prospective study. Head Neck 2003;25:864–72.
[38] Li Z, Ren Y, Lin SX, Liang YJ, Liang HZ. Association of E-cadherin and beta-catenin with metastasis in nasopharyngeal carcinoma. Chin Med J (Engl) 2004;117:1232–9.
[39] Zhang ZB, Cai L, Zheng SG, Xiong Y, Dong JH. Overexpression of caveolin-1 in hepatocellular carcinoma with metastasis and worse prognosis: correlation with vascular endothelial growth factor, microvessel density and unpaired artery. Pathol Oncol Res 2009.
[40] Kato K, Hida Y, Miyamoto M, Hashida H, Shinohara T, Itoh T, et al. Over-expression of caveolin-1 in esophageal squamous cell carcinoma correlates with lymph node metastasis and pathologic stage. Cancer 2002;94:929–33.
[41] Campbell L, Jasani B, Edwards K, Gumbleton M, Griffiths DF. Combined expression of caveolin-1 and an activated AKT/mTOR pathway predicts reduced disease-free survival in clinically confined renal cell carcinoma. Br J Cancer 2008;98:931–40.
[42] Thompson TC. Metastasis-related genes in prostate cancer: the role of caveolin-1. Cancer Metastasis Rev 1998;17:439–42.
[43] Du ZM, Hu CF, Shao Q, Huang MY, Kou CW, Zhu XF, et al. Upregulation of caveolin-1 and CD147 expression in nasopharyngeal carcinoma enhanced tumor cell migration and correlated with poor prognosis of the patients. Int J Cancer 2009;125:1832–41.
[44] Hsu HK, Juan SH, Ho PY, Liang YC, Lin CH, Teng CM, et al. YC-1 inhibits proliferation of human vascular endothelial cells through a cyclic GMP-independent pathway. Biochem Pharmacol 2003;66:263–71.
[45] Chiang WC, Teng CM, Lin SL, Chen YM, Tsai TJ, Hsieh BS. YC-1-inhibited proliferation of rat mesangial cells through suppression of cyclin D1-independent of cGMP pathway and partially reversed by p38 MAPK inhibitor. Eur J Pharmacol 2005;517:1–10.
[46] Wong N, Hui AB, Fan B, Lo KW, Pang E, Leung SF, et al. Molecular cytogenetic characterization of nasopharyngeal carcinoma cell lines and xenografts by comparative genomic hybridization and spectral karyotyping. Cancer Genet Cytogenet 2003;140:124–32.
[47] Ma BB, Lui VW, Poon FF, Wong SC, To KF, Wong E, et al. Preclinical activity of gefitinib in non-keratinizing nasopharyngeal carcinoma cell lines and biomarkers of response. Invest New Drugs; in press.
[48] Miller WE, Earp HS, Raab-Traub N. The Epstein-Barr virus latent membrane protein 1 induces expression of the epidermal growth factor receptor. J Virol 1995;69:4390–8.